Article

Immunity

Adipose Type One Innate Lymphoid Cells Regulate Macrophage Homeostasis through Targeted Cytotoxicity

Graphical Abstract

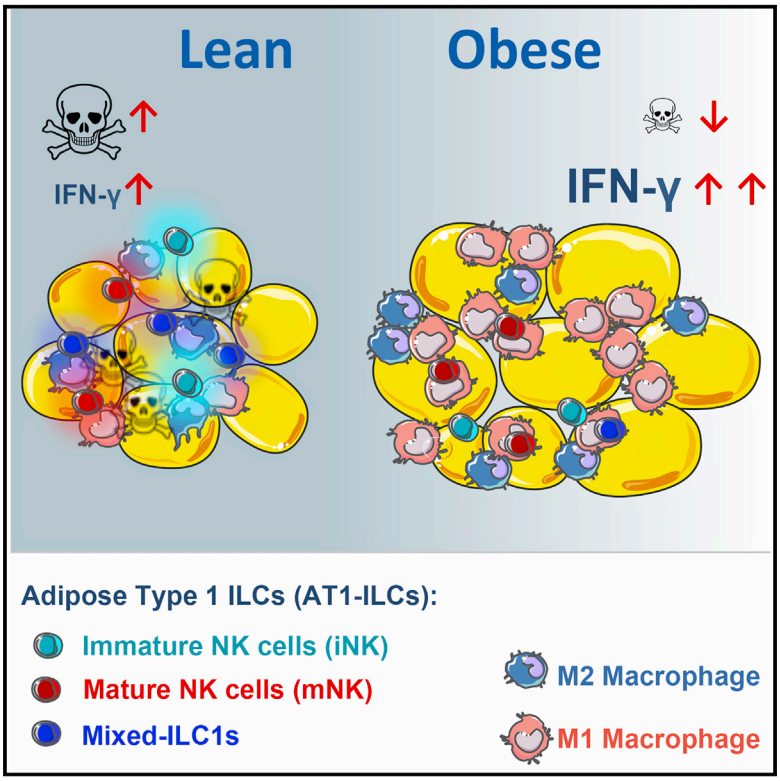

Authors

Selma Boulenouar, Xavier Michelet, Danielle Duquette, ..., Michael B. Brenner, Ulrich von Andrian, Lydia Lynch

Correspondence

llynch@bwh.harvard.edu

In Brief

Boulenouar et al. define different subsets of type 1 innate lymphoid cells (AT1-ILCs) in human and murine adipose tissues and show that at steady state, AT1-ILCs kill adipose tissue macrophages (ATMs). In obesity, cytotoxicity is impaired. Interference with AT1-ILC cytotoxicity impacted ATM homeostasis and systemic metabolism, pointing to its importance in homeostasis and disease.

Highlights

- AT1-ILCs are enriched in mouse and human adipose tissue and are predominantly tissue resident
- AT1-ILCs kill adipose tissue macrophages (ATMs) and maintain ATM homeostasis
- Subsets of AT1-ILCs infiltrate adipose tissue during the onset of obesity
- In obesity, AT1-ILCs are reduced and lose their ability to kill

Boulenouar et al., 2017, Immunity *46*, 273–286
February 21, 2017
http://dx.doi.org/10.1016/j.immuni.2017.01.008

Immunity
Article

Adipose Type One Innate Lymphoid Cells Regulate Macrophage Homeostasis through Targeted Cytotoxicity

Selma Boulenouar,[1,2] Xavier Michelet,[1,2] Danielle Duquette,[1] David Alvarez,[2] Andrew E. Hogan,[3] Christina Dold,[4] Donal O'Connor,[3] Suzanne Stutte,[2] Ali Tavakkoli,[1] Desmond Winters,[3] Mark A. Exley,[1] Donal O'Shea,[3] Michael B. Brenner,[1] Ulrich von Andrian,[2] and Lydia Lynch[1,2,4,5,*]
[1]Brigham and Women's Hospital, Boston, MA 02115, USA
[2]Harvard Medical School, Boston, MA 02115, USA
[3]Education Research Centre, St. Vincent's University Hospital, Dublin 4, Ireland
[4]School of Biochemistry and Immunology, Trinity Biomedical Sciences Institute, Trinity College Dublin, Dublin 2, Ireland
[5]Lead Contact
*Correspondence: llynch@bwh.harvard.edu
http://dx.doi.org/10.1016/j.immuni.2017.01.008

SUMMARY

Adipose tissue has a dynamic immune system that adapts to changes in diet and maintains homeostatic tissue remodeling. Adipose type 1 innate lymphoid cells (AT1-ILCs) promote pro-inflammatory macrophages in obesity, but little is known about their functions at steady state. Here we found that human and murine adipose tissue harbor heterogeneous populations of AT1-ILCs. Experiments using parabiotic mice fed a high-fat diet (HFD) showed differential trafficking of AT1-ILCs, particularly in response to short- and long-term HFD and diet restriction. At steady state, AT1-ILCs displayed cytotoxic activity toward adipose tissue macrophages (ATMs). Depletion of AT1-ILCs and perforin deficiency resulted in alterations in the ratio of inflammatory to anti-inflammatory ATMs, and adoptive transfer of AT1-ILCs exacerbated metabolic disorder. Diet-induced obesity impaired AT1-ILC killing ability. Our findings reveal a role for AT1-ILCs in regulating ATM homeostasis through cytotoxicity and suggest that this function is relevant in both homeostasis and metabolic disease.

INTRODUCTION

The last decade has revealed that adipose tissue (AT) is not just an inert energy storage tissue but is essential for metabolic health through the production of a diverse array of adipokines and due to the unique adipose-resident immune system (Exley et al., 2014; Kanneganti and Dixit, 2012). A key feature of AT is its ability to respond to changes in nutrient fluctuations, expanding and contracting to deal with changes in energy intake (Rosen and Spiegelman, 2014). It is now clear that the adipose immune system plays an important role in adipose homeostasis. In the lean state, adipose tissue is enriched with regulatory cells including Treg cells, regulatory iNKT cells, eosinophils, type 2 innate lymphoid cells (ILC2s), and alternatively activated "M2" macrophages (Brestoff et al., 2015; Feuerer et al., 2009; Lynch et al., 2009a, 2012; Wu et al., 2011). This regulatory immune system is critical for maintaining a metabolically healthy state and for keeping inflammation at bay during tissue fluctuations (Exley et al., 2014). The adipose response to excess energy or fasting can trigger a local immune response, and this needs to be kept in check to prevent aberrant responses and damage. In obesity, there is an immune response to excess energy, which subsequently contributes to metabolic disorder. Adipocyte hypertrophy in obesity leads to lipid release, stress signals, and chemokines that attract and activate "M1" macrophages and other pro-inflammatory immune cells (Lumeng et al., 2007). At the same time, the adipose-resident regulatory immune cells are lost, leading to uncontrolled chronic inflammation (Feuerer et al., 2009; Ji et al., 2012; Lynch et al., 2009a, 2012; Schipper et al., 2012). This response contributes to local and systemic increases in pro-inflammatory cytokines like TNF-α, which interfere with insulin signaling leading to insulin resistance (Hotamisligil et al., 1993; Kahn and Flier, 2000). Much research has focused on this harmful inflammatory response, but less is known about the resident immune system in steady state that likely plays critical functions in normal adipose homeostasis. Furthermore, it is often forgotten that the physiological response of adipose tissue macrophages (ATMs) and other immune cells is likely beneficial in the early stage of obesity. For example, ATMs provide a buffering protection against lipotoxicity through uptake of free lipids that would be toxic locally and systemically (Fischer-Posovszky et al., 2011; Xu et al., 2013). Lipid-filled ATMs also accumulate during fasting, caloric restriction, and pharmacologically induced lipolysis, suggesting that ATMs are an important physiological response to perturbations in adipose tissue (Kosteli et al., 2010; Sun et al., 2011). Understanding the adipose-resident immune system at steady state is important for our appreciation of adipose immunity and for preventing inflammation-induced metabolic disorder.

Recently, type 1 innate lymphoid cells (T1-ILCs), including their founding member, natural killer (NK) cells, joined the dynamic immune response that occurs in AT in response to obesity

(Lee et al., 2016; O'Sullivan et al., 2016; Wensveen et al., 2015). Adipose T1-ILCs (AT1-ILCs) played a pathogenic role by promoting pro-inflammatory M1 macrophages that underlie obesity-associated insulin resistance. However, T1-ILCs represent a major component of the adipose lymphoid compartment at steady state, and their role in lean AT has not been studied. In addition, it is unknown whether T1-ILCs interact with macrophages at steady state in lean mice, when the majority of ATMs are anti-inflammatory tissue repair-associated M2 phenotype. Indeed, NK cells and macrophages can cooperate to clear infections in many tissues. Macrophages and monocytes can activate NK cells through soluble factors (i.e., IL-12 and IL-18) and NK cells secrete IFN-γ which potentiates macrophage/monocytes activation (Michel et al., 2013). NK cells can kill endogenous infected or LPS-activated macrophages, likely preventing further damage to the host (Lapaque et al., 2009; Nedvetzki et al., 2007). However, it is now appreciated that T1-ILCs are expanding and NK cells are no longer the sole component of this group. Diverse ILC1s are frequently identified in different tissues and can be also classified as T1-ILCs (Cortez and Colonna, 2016; Seillet and Belz, 2016; Spits et al., 2016). In murine adipose tissue, using GFP-reporter mice, three major AT1-ILC populations were recently identified: (1) mature NK (mNK) cells, (2) immature NK (iNK) cells, and (3) ILC1s. ILC1s were reported to be the major contributors for IFN-γ upregulation during diet-induced obesity resulting in the expansion of pro-inflammatory M1 macrophages (O'Sullivan et al., 2016), similar to the previous report on the role of adipose NK cells in obesity (Wensveen et al., 2015). However, the precise interaction between each AT1-ILC subsets with macrophages at steady state and during obesity remains unclear.

Here, we examined human and murine adipose tissue and found heterogeneous populations of AT1-ILCs. Based on the expression of surface cell markers, transcription factors, cytokines, and cytotoxicity signatures that define type 1 ILCs, we identified three major subsets in mouse and two subsets in human adipose tissue. These subsets displayed distinct trafficking characteristics and differential plasticity in lean and obese states and after weight loss. We examined each AT1-ILC subset at steady state and found that all subsets displayed cytotoxic activity toward ATM. This killing ability was impaired during obesity and could contribute to the skewing toward a pathogenic accumulation of pro-inflammatory macrophages.

RESULTS

Type 1 ILCs Are Enriched in Human and Mouse Adipose Tissues and Are Predominantly Tissue Resident

Recent reports have shown that AT has a substantial immune system with an enrichment of innate immune cells (Brestoff and Artis, 2015; Exley et al., 2014). Most recently, NK cells and other T1-ILC subsets have been described in murine adipose tissue in obesity (Lee et al., 2016; O'Sullivan et al., 2016; Wensveen et al., 2015). Little is known about T1-ILCs in adipose tissue at steady state in mice and humans. In humans, different T1-ILCs were identified in lymphoid and non-lymphoid peripheral tissues based on the lack of c-Kit and ROR-γt (Björkström et al., 2016; Spits et al., 2016). We found that $CD56^{+}CD3^{-}$ cells in human adipose tissue do not express c-Kit and ROR-γt (Figure S1A) and we identified them as T1-ILCs. In visceral omental fat, T1-ILCs were enriched (7%–20% of omental lymphocytes) compared to matched blood (5%–12% of peripheral lymphocytes; Figure 1A). To investigate whether T1-ILC enrichment was specific to omentum, we collected samples from four distinct adipose compartments from seven non-obese individuals undergoing abdominal surgery. All human adipose depots examined contained substantial levels of T1-ILCs (~5%–10% of resident lymphocytes; Figure 1B), although omentum has the highest frequency and number (Figures 1B and 1C).

In mice, epididymal white adipose tissue (WAT) was highly enriched with $NK1.1^{+}CD3^{-}$ cells at steady state, showing the highest frequency among all organs tested (Figures 1D and S1B). Recently, adipose $NK1.1^{+}Lin^{-}$ cells were identified as T1-ILCs that expressed T-bet and showed no history of ROR-γt expression (O'Sullivan et al., 2016). It was also shown earlier that in obesity, adipose $NK1.1^{+}CD3^{-}$ cells did not express other ILCs receptor/markers such as IL-7R-α and c-Kit (Wensveen et al., 2015). Here, we report that at steady state, murine T1-ILCs constituted 22%–30% of adipose lymphocytes, compared to 7% in blood, 3% in spleen and peritoneal fluid, ~12% in liver, <1% in the lymph node and thymus, and ~5% in bone marrow (Figures 1D and S1B). We also found significant proportions of T1-ILCs in all other adipose depots examined, including brown adipose tissue (BAT), peri-renal, mesenteric, and sub-cutaneous adipose tissue, although the highest levels were seen in epididymal and female parametrial depots (Figure S1C). T1-ILCs were not only enriched in adipose tissue compared to other sites, but also were the most abundant lymphocyte population in adipose tissue (Figure 1E). Similar findings were seen in BALB/c mice (data not shown), suggesting their enrichment is not refined to one mouse strain. T1-ILCs levels fluctuated with age, with peak levels between 8 and 30 weeks old, which declined to significantly lower levels in 1-year-old animals (Figure 1F).

We then asked whether adipose T1-ILCs were resident or constantly recirculating through adipose from the periphery. We generated parabiotic mice with congenic CD45.1 and CD45.2 mice. During the healing process after surgery, capillary anastomoses form between the two vascular systems, allowing for exchange of circulating peripheral blood cells. After 2 weeks of parabiosis, T1-ILCs recirculated completely in the blood and spleen between the two parabiotic partners (Figure 1G). T1-ILCs in liver circulated less, reaching ~30% chimerism, confirming previous findings (Sojka et al., 2014). However, only about one-fifth of adipose T1-ILCs were partner derived (Figure 1G). To confirm that low chimerism of T1-ILCs in adipose tissue was not due to low circulation dynamics of all adipose lymphocytes, we compared T1-ILC recirculation to other lymphocyte populations in adipose tissue. B cells and CD8 T cells completely recirculated through adipose tissue, reaching levels that approach 50% chimerism, indicating almost full exchange (Figure 1H). Our findings suggest that T1-ILCs are enriched in adipose tissue where they are largely resident and rely less on infiltration from the periphery, unlike spleen where they constantly recirculate.

Unique T1-ILC Subsets Populate Mouse Adipose Tissue at Steady-State

Given that T1-ILCs display a more resident phenotype than elsewhere, we hypothesized that they might have a distinct adipose

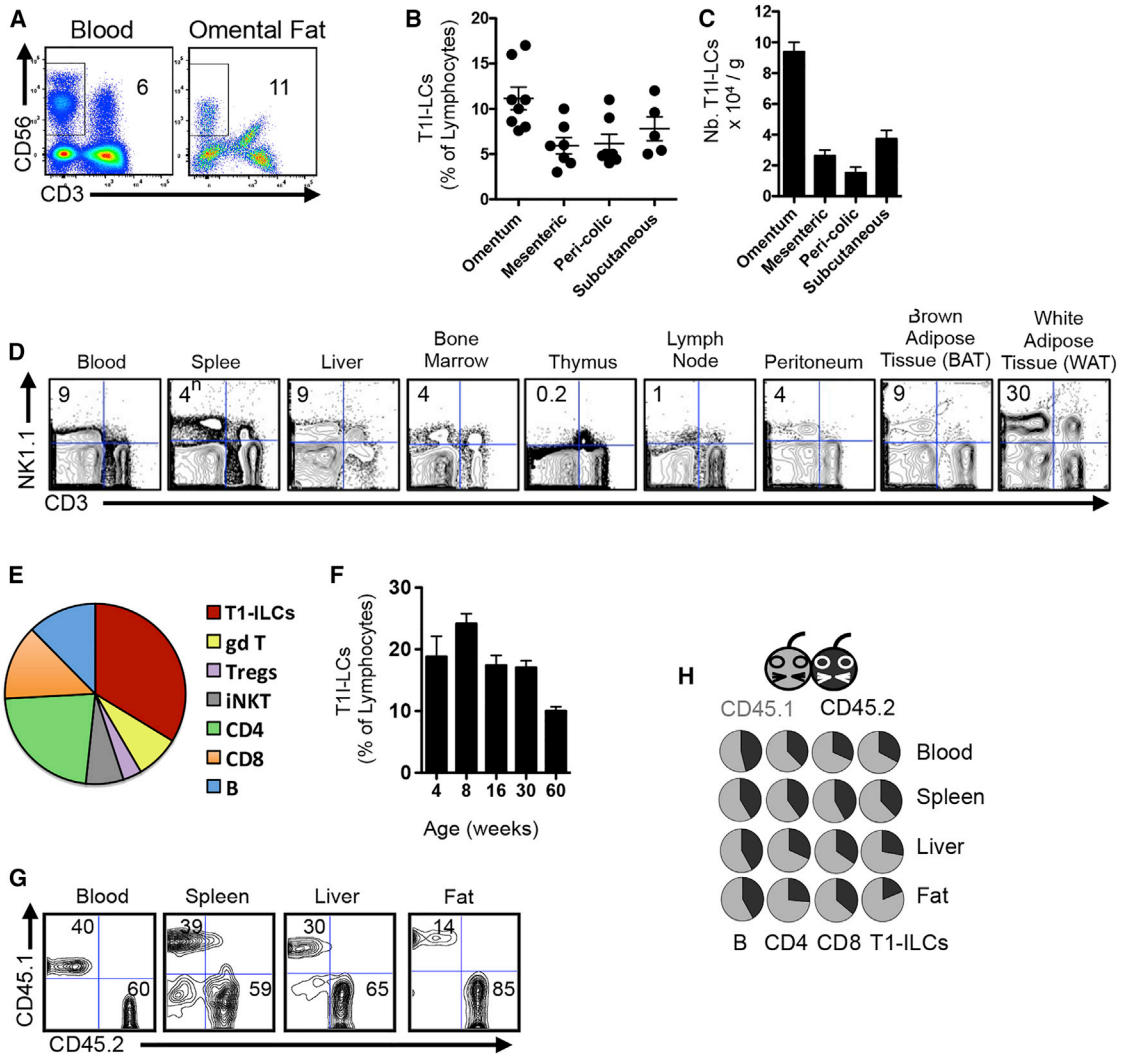

Figure 1. Adipose AT1-ILCs Are Enriched in Human and Mouse Adipose Tissues

(A) Representative flow cytometry plots of human AT1-ILC CD56^{+}CD3^{-} cells in matched blood and omental adipose tissue.

(B and C) T1-ILCs levels (B) and recovered numbers (C) in human matched adipose tissue depots (n = 5–8 per sample).

(D) Representative contour plots of mouse T1-ILCs (NK1.1^{+}CD3^{-}) in matched blood, liver, spleen, peritoneal fluid, bone marrow (BM), thymus, peripheral lymph node, brown adipose tissue (BAT), and white epididymal adipose tissue (WAT) in WT C57BL/6 mice.

(E) Pie chart indicates the proportions of all lymphocyte populations in murine epididymal tissue in 6- to 8-week-old C57BL/6 mice.

(F) Graphs of mouse T1-ILCs (NK1.1^{+}CD3^{-}) in adipose tissue in young and aged C57BL/6 mice (4–60 weeks).

(G) CD45.1 and CD45.2 congenic mice were joined in parabiotic pairs (5 pairs) at 6 weeks of age for 3 weeks. Representative FACS dot plots gated on T1-ILCs from blood, spleen, liver, and fat of the CD45.1 member of a parabiotic pair after 15 days of parabiosis show the relative frequencies of CD45.1 (host) and CD45.2 (parabiotic partner) T1-ILCs in each organ.

(H) Pie charts indicate the average of the relative frequencies of CD45.1 (gray) and CD45.2 (black) cells from 5 parabiotic pairs after 15 days in CD45.1 partner of each pair.

Error bars represent SEM. Statistical comparisons using unpaired two-tailed Student's t test. *$p < 0.05$, **$p \leq 0.01$, ***$p < 0.001$. See also Figure S1.

phenotype. Unusually, the majority of AT1-ILCs expressed low or no Ly49 markers, suggesting that they are uneducated (Figure S2A). However, the bimodal expression profile of Thy1 and NKG2A (Figure S2A) prompted us to question whether AT1-ILCs comprised heterogeneous subsets. Hence, we performed an in-depth phenotypic analysis. Tissue-resident ILC1s are distinguished from circulating cNK cells in several tissues including liver, skin, salivary glands (Cortez et al., 2014), and uterus by the expression of CD49a and DX5 markers (Boulenouar et al., 2016; Peng et al., 2013; Sojka et al., 2014). First, based on CD49a and DX5 surface expression, we identified that AT1-ILCs (NK1.1^{+}NKp46^{+}CD3) are made up of four subsets which we have annotated as double negative (DN, DX5^{-}CD49a^{-}), ILC1-like (DX5^{-}CD49a^{+}), double positive (DP, DX5^{+}CD49a^{+}), and conventional (cNK, DX5^{+}CD49a) NK cells (Figure 2A). The composition of T1-ILC subsets was unique in adipose tissue. cNK cells were much fewer (30%), while DN and ILC1-like subsets were enriched, and a DP population

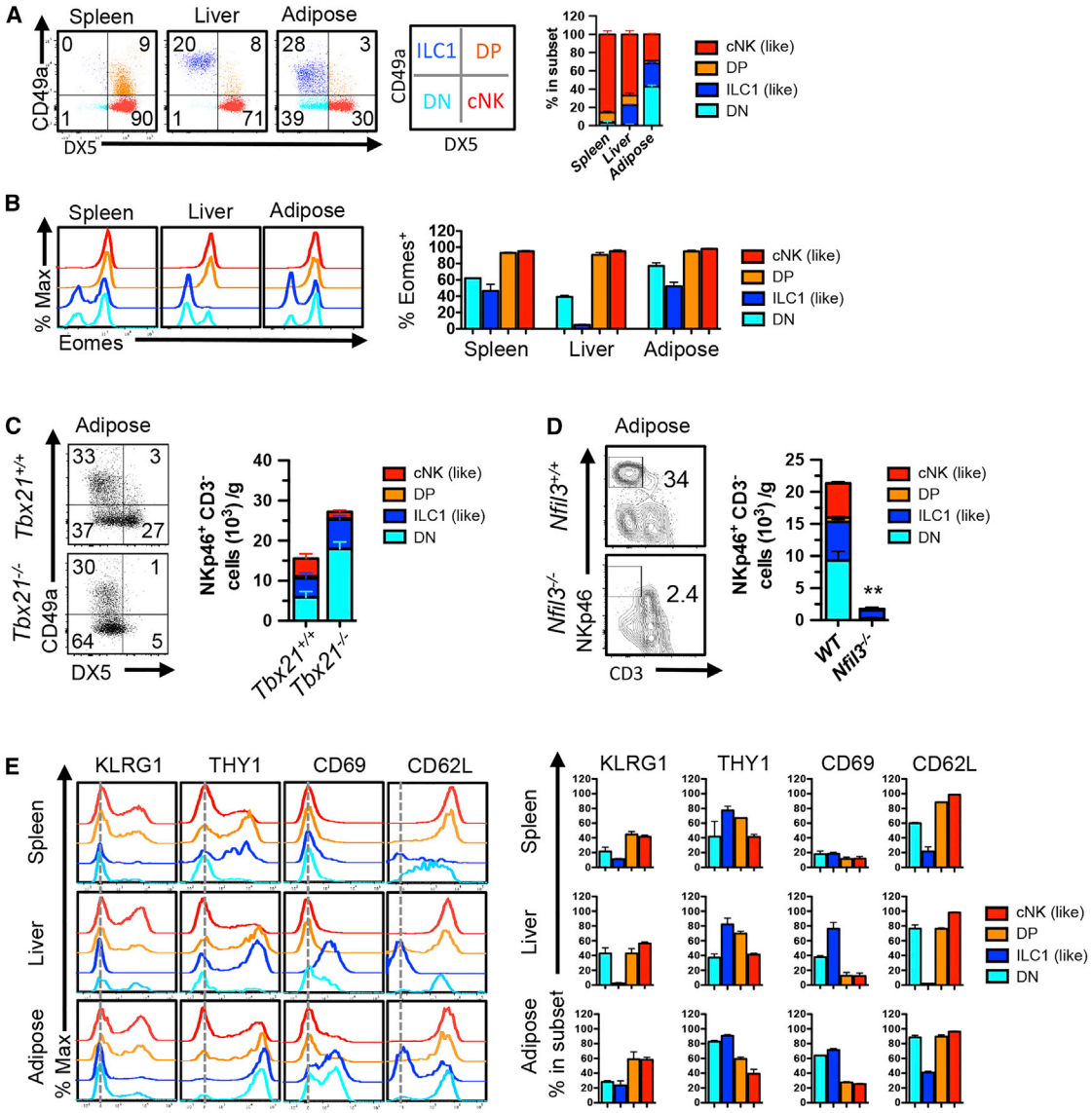

Figure 2. Unique T1-ILC Subsets Populate Mouse Adipose Tissue at Steady State and Are Distinct from Spleen and Liver ILC1s

(A) Representative flow cytometry plots showing separation of CD45$^+$CD3$^-$NK1.1$^+$NKp46$^+$ T1-ILCs using CD49a and DX5$^-$ cell surface markers into double negative (DN), innate lymphoid type 1 like (ILC1), double positive (DP) and conventional NK cells (cNK) in spleen, liver, and epididymal adipose with descriptive diagram naming each subset in the quadrant (right).

(B) Representative cytometry histograms of Eomesodermin (Eomes) expression in T1-ILCs subsets.

(C) Representative cytometry plots of NKp46$^+$CD3$^-$ T1-ILC subsets in adipose tissue from *Tbx21*$^{+/+}$ and *Tbx21*$^{-/-}$ mice.

(D) Representative cytometry plot of T1-ILCs in adipose from *Nfil3*$^{-/-}$ and *Nfil3*$^{+/+}$ mice.

(E) Histograms of cell surface expression of tissue residency-associated (CD69), activation, and maturation (CD62L, Thy1, and KLRG1) markers.

Error bars represent SEM. Data representative of two to three independent experiments, n = 2–5 mice per group. Statistical comparisons by unpaired two-tailed Student's t test. *p < 0.05, **p ≤ 0.01, ***p < 0.001. See also Figure S2.

were found at residual level (<5%). In contrast, splenic cNK cells represented the majority (>90%) of NK cells, while in liver, cNK cells and ILC1 populations represented ~70% and ~25%, respectively, as previously reported (Figure 2A; Sojka et al., 2014).

Deciphering the biology of T1-ILCs is a fast-evolving topic and subset-specific markers are frequently updated. In mice, the current standard is to examine their capacity to produce IFN-γ and their developmental requirement of T-bet. More recently, the use of *Eomes* (Eomesodermin) reporter mice showed differential expression of Eomes and T-bet by cNK cells and ILC1s (Daussy et al., 2014). Eomes$^+$ ILC1s (cNK cells) is distinguished from Eomes$^-$ ILC1s derived from distinct precursors (Cortez and Colonna, 2016; Seillet and Belz, 2016; Serafini et al., 2015). However, the identification of salivary gland Eomes$^+$ ILC1s is an exception to this rule (Cortez et al., 2014, 2016). Here,

we analyzed intracellular expression of Eomes in each subset in spleen, liver, and adipose (Figure 2A, middle). As expected, the majority of T1-ILCs in spleen were Eomes$^+$, and the ILC1 subset in liver was Eomes$^-$ as previously reported (Daussy et al., 2014; Gordon et al., 2012; Sojka et al., 2014). In adipose, cNK cells and DP AT1-ILCs expressed Eomes at levels similar to splenic and hepatic cNK cells. However, a significant fraction of DN and ILC1-like subsets did not express Eomes (~15% and ~60%, respectively, Figure 2B), suggesting heterogeneous transcriptional programming. Next, we determined the developmental dependency on Tbet for each AT1-ILC subset using Tbet-deficient (*Tbx21*$^{-/-}$) mice and found that the frequency and the density of cNK and DP cell subsets were dramatically decreased while DN cells were significantly increased in AT, compared to *Tbx21*$^{+/+}$ mice. However, the level of ILC1-like subset was not affected by the absence of *Tbx21* (Figures 2C and S2B). This differential requirement for *Tbx21* for AT1-ILC subsets was similar in BAT (Figure S2C). Remarkably, we found that ILC1-like subset was predominantly Eomes$^+$ in *Tbx21*$^{-/-}$ mice and that all Eomes$^-$ cells were depleted in adipose and elsewhere (Figure S2D). Similar to Sun et al. (2011), we found that Eomes$^-$ AT1-ILCs are strictly dependent on *Tbx21* unlike the Eomes$^+$DX5$^-$ identified as immature NK (iNK) cells that double in frequency in the absence of *Tbx21* (Figure S2E, top; O'Sullivan et al., 2016). However, we also found that in *Tbx21*$^{-/-}$ mice, the percent of CD49a$^+$ cells is increased 2-fold within the iNK cell subset (Figures 2C and S2E). In WT mice, CD49a$^+$ is a mixed population composed of Eomes$^+$ iNK cells and Eomes$^-$ ILC1s. The expansion of Eomes$^+$ iNK cells in *Tbx21*$^{-/-}$ mice suggest that iNK cells could acquire some attributes of ILC1s such as the expression of CD49a to maintain the presence of this subset at the physiological level.

Next, we examined the dependency on the transcription factor *Nfil3*, which encodes Nuclear Factor Interleukin-3 (E4BP4). The developmental requirement on *Nfil3* is different among T1-ILCs subsets in each tissue, with cNK cells requiring *Nfil3* for development while other ILC populations do not (Diefenbach et al., 2014; Serafini et al., 2015). Here, using *Nfil3*$^{-/-}$ and littermate control *Nfil3*$^{+/+}$ mice, we found that the percentage of total AT1-ILCs was dramatically reduced (~15-fold decrease, Figures 2D and S2F) as were cNK cells in blood in *Nfil3*$^{-/-}$ mice. Thus, AT1-ILC subsets are uniformly dependent on *Nfil3*.

We next investigated the maturation level of each AT1-ILCs subset, based on the expression of CD27 and CD11b. NK cell maturation is a 4-stage process that begins at CD11b^{lo} CD27^{lo} (stage 1), followed by the proliferative stage which are CD11b^{lo}CD27^{hi} (stage 2). In stage 2, NK cells start to acquire their NK cell receptor repertoire and in stage 3 (CD11b^{hi}CD27^{hi}) and stage 4 (CD11b^{hi}CD27^{lo}), they acquire their full effector potential (diagram in Figure S2G, bottom; Chiossone et al., 2009). Interestingly, we found that each of the AT1-ILC subsets had a distinct maturation level (Figure S2G). The least mature subsets were the adipose ILC1-like subset and the DN subset (stage 2/3), while the DP subset was at intermediate maturation stage 3. Finally, cNK cells were mainly terminally differentiated cells (~65% CD11b$^+$), compared to the cNK cells in spleen and liver, which expressed lower levels of CD11b$^+$ cells (~35% and 50%, respectively). KLRG1 expression can also mark terminal maturation in NK cells (Vosshenrich et al., 2005), and adipose DP and cNK cells also expressed more KLRG1 compared to DN and ILC1-like cells. KLRG1 expression inversely correlated with Thy1 expression, a marker associated with early development of NK cells. Thus, the maturation profile of AT1-ILCs is heterogeneous, distinct from liver and spleen, and comprises a large proportion of "immature-like" cells. Activated NK cells upregulate early activation marker CD69 and downregulate L-Selectin (CD62L) (Diefenbach et al., 2014), which are also features of tissue residency. Adipose ILC1-like and DN NK cells expressed higher levels of CD69 than DP and cNK cells. However, unlike hepatic ILC1s, all AT1-ILC subsets expressed CD62L (Figure 2E). Combined, we define AT1-ILCs as *Nfil3* dependent and composed of subsets with differential requirement and expression of Tbet and Eomes. Thus, to align with up-to-date nomenclature (O'Sullivan et al., 2016), we designate three major AT1-ILC subsets as DN subset as immature NK (iNK); CD49a$^+$ ILC1-like subset (mixed ILC1s); and cNK subset as mature NK (mNK), in addition to a minor DP subset (Figure S2H).

Distinct Effector and Trafficking Properties for Mouse Adipose NK Cell Subsets

T1-ILCs are characterized by their cytotoxic potential and their capacity to produce IFN-γ (Cortez and Colonna, 2016; Seillet and Belz, 2016; Serafini et al., 2015). We next explored effector functions and found that adipose iNK cell and mixed ILC1 subsets expressed very little granzyme B unlike mNK cells. Interestingly, unlike hepatic ILC1s, adipose mixed ILC1 subsets are devoid of TNF-α receptor TRAIL and express granzyme B at low levels (Figure 3A). To investigate IFN-γ production in vivo, we used IFN-γ-reporter mice (*Ifng*$^{tm3.1Lky}$) (Reinhardt et al., 2009). All AT1-ILC subsets expressed IFN-γ but mixed ILC1 population expressed the highest level of IFN-γ, compared to mNK cells (Figure 3B). As previously shown (Figures 1G and 1H), AT1-ILCs are predominantly resident. The heterogeneous nature of adipose NK cells led us to further examine the trafficking characteristics of each subset in adipose tissue. Using parabiosis, we found that mNK cells recirculate through adipose, evidenced by almost total chimerism (~50% in each parabiont). In stark contrast, there was very little recirculation in the DP, mixed ILC1, and iNK cell populations, indicating that they are predominantly resident. This was also in contrast to the equivalent populations (albeit found at negligible levels) in the spleen (Figure 3C). Collectively, our findings indicate that the adipose NK cell pool is comprised of unique AT1-ILCs, including tissue-resident iNK, mixed ILC1 and DP cells, and a minor circulating mNK subset, and that each subset has distinct transcriptional programming, maturation levels, activation, and effector functions.

Human Adipose Tissue Contains Distinct ILC Group 1 Subsets

The study of human ILCs remains technically challenging due to some ambiguity in the phenotypic and functional definition of each subset and to the heterogeneity of T1-ILCs among different tissues and organs (Björkström et al., 2016; Spits et al., 2016). Little is known about T1-ILCs, including NK cells, in human adipose. We analyzed matched blood and visceral omental adipose tissue from previously obese patients undergoing abdominal

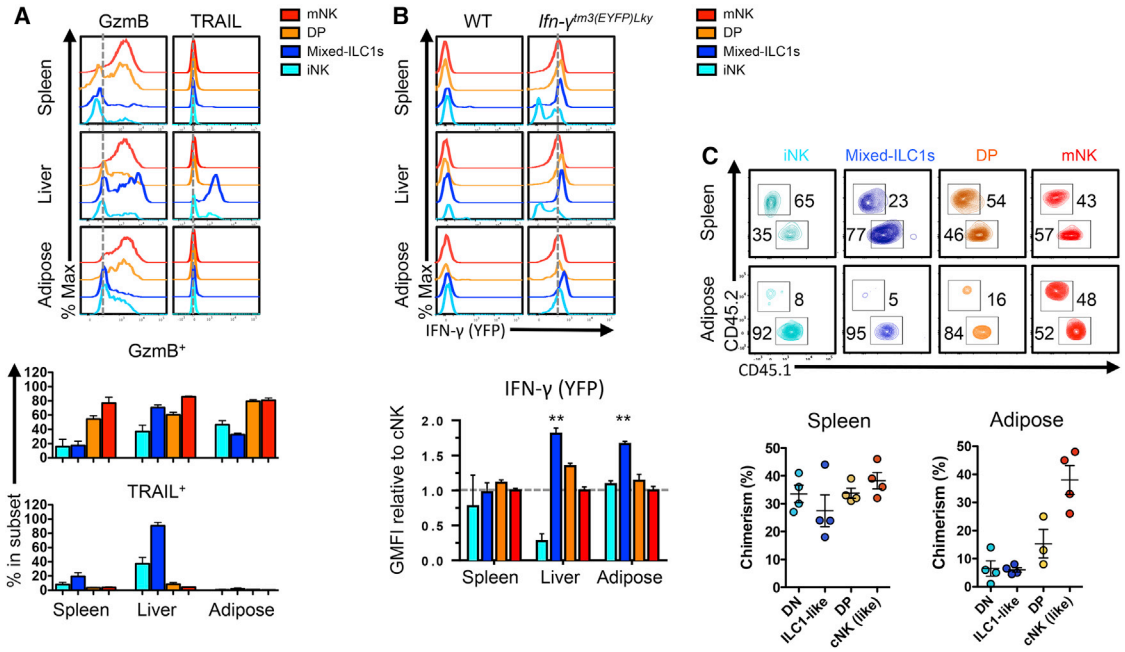

Figure 3. Distinct Effector Signatures between Adipose DX5$^-$CD49a$^+$ ILC1-like and DX5$^-$CD49a$^-$ DN Cells yet Both Are Tissue Resident

(A) Representative cytometry histograms (top) and quantitation (bottom), percentages of Granzyme B$^+$ (GrzmB) and the death receptor TRAIL$^+$ cells in each T1-ILCs subset in matched spleen, liver, and adipose.

(B) Representative cytometry histograms (top) and quantitation (bottom) of *Ifng*$^{tm3(EYFP)Lky}$; results are normalized to those of conventional NK cells subset in matched spleen, liver, and adipose.

(C) Parabiotic mice: Contour plots gated on NK cell subsets (DN, ILC1-like, DP, and cNK) from spleen and adipose of the CD45.1 member of a parabiotic pair after 15 days of parabiosis show the relative frequencies of CD45.1 (host) and CD45.2 (parabiotic partner) T1-ILC subsets in each tissue. Graph of chimerism of T1-ILCs subsets in each organ.

Data representative of 2–3 independent experiments, n = 2–5 mice per group, and parabiosis: 5 pairs. Error bars represent SEM. Statistical comparisons using unpaired two-tailed Student's t test. *p < 0.05, **p ≤ 0.01, ***p < 0.001.

plastic surgery. Human peripheral blood typically contains CD56^{bright}CD16$^+$ (95%) and CD56^{dim}CD16$^-$ (5%) NK cells, which are functionally distinct. We consistently found that human adipose is devoid of CD56^{bright} subset. Almost half of the CD56^{dim} subset did not express CD16, unlike in blood (Figure 4A). Adipose CD56^{dim}CD16$^+$ cells were predominantly CD127$^-$CD161$^+$, characteristic of peripheral NK (pNK) cells, but expressed Eomes at lower levels. The CD56^{dim}CD16$^-$ subset expressed very low levels of CD127 and higher levels of CD161 and did not express Eomes, which is a similar phenotype to a tonsil and gut CD127$^+$ ILC1 population recently described (Bernink et al., 2013, 2015), with an important distinction of CD56 expression in adipose that was not reported in tonsil and gut ILC1s (Figure 4B). In addition, CD69 was expressed at higher levels, suggesting a more activated state and residency signature compared to blood (Figure 4C). We also found differential cytotoxic potential between the two AT1-ILCs subsets, where CD56^{dim}CD16$^-$ NK cells expressed significantly less granzyme B and Perforin, another common feature of CD127$^+$ ILC1s, compared to higher levels of perforin and granzyme B in the CD56^{dim}CD16$^+$ pNK-like subset (Figure 4E). Hence, like murine adipose tissue, we describe novel human AT1-ILCs subsets including a CD56$^+$CD127^{lo} ILC1-like population that is enriched in human adipose that appears to have less cytotoxic potential in resting conditions.

AT1-ILCs Dynamically Respond and Adapt to Changes in Diet in Humans and Mice

One of the unique features of AT is its plasticity to rapidly expand and contract in response to changes in energy supply through the diet (Rosen and Spiegelman, 2014). Recent studies have shown that several immune subsets in adipose tissue also respond to changes in diet (Exley et al., 2014). In mice, it was recently reported that AT1-ILC absolute numbers increased in obesity (4–12 weeks high-fat diet [HFD]) (Lee et al., 2016; Wensveen et al., 2015); however, recent work reported that their density remained unchanged (O'Sullivan et al., 2016). We first asked how AT1-ILCs in humans respond to obesity and weight loss. We have previously shown that NK cell levels are severely reduced in the blood of patients with obesity, compared to lean age-matched controls (Lynch et al., 2009b). Here, we found that obese omental adipose tissue has a lower frequency of AT1-ILCs compared to lean omental tissue in humans (~12% versus ~5%; Figure 5A). Next, we asked whether weight loss would alter the T1-ILCs levels in the periphery by looking cross-sectionally at patients before and after bariatric surgery. Confirming our previous findings, we found reduced levels of T1-ILCs in obese patients (BMI > 40) compared to lean controls in a cross-sectional study. However, T1-ILCs levels significantly increased 18 months after bariatric surgery, when BMI was significantly lower, although still in the obese range (Figure 5B). We also

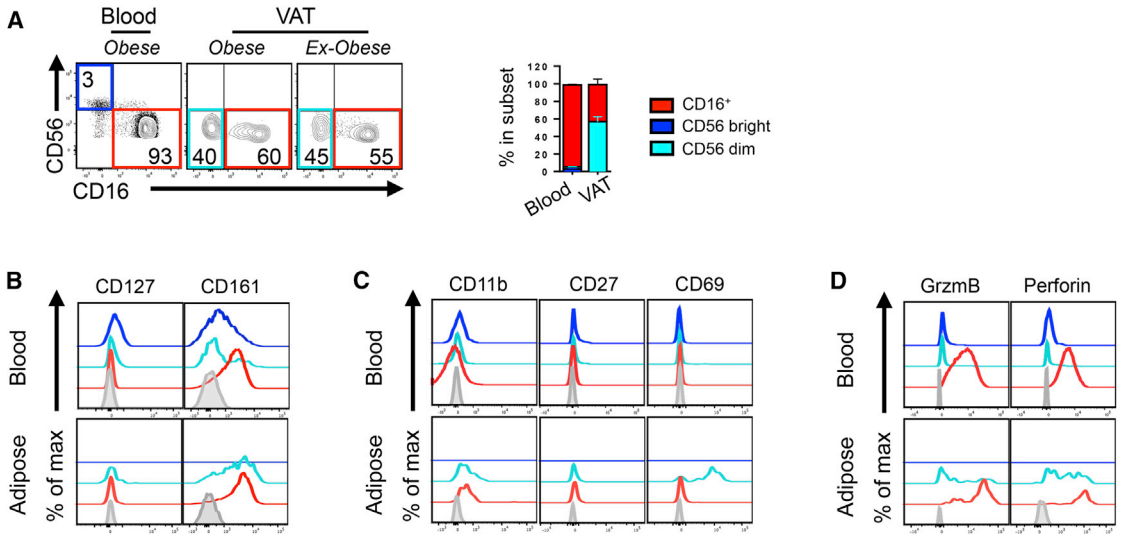

Figure 4. Human Adipose Tissue Is Enriched with Unique CD56^{dim}CD16^{-} NK Cell Subset with Poor Cytotoxic Potential in Obesity

(A) Representative flow cytometry plots of human T1-ILCs subsets in matched blood and omental adipose tissue from obese and ex-obese individuals (n = 6). Error bars represent SEM.

(B–D) Histograms of (B) development, (C) maturation/activation, and (D) cytotoxicity in matched blood and omental adipose of obese individuals.

followed six patients longitudinally and found that there was a significant increase in T1-ILCs in each patient after weight loss through bariatric surgery (~5% versus ~10%; Figure 5B, left). Thus, we found that AT1-ILC levels are reduced during chronic obesity but could recover to near normal levels upon restricted food intake in humans. Next, we conducted a more detailed analysis on mice to follow the dynamics of AT1-ILCs at the onset of obesity. Within the first 96 hr of starting a HFD, during which time the mice are not yet obese but have significantly larger epididymal fat pads, AT1-ILC frequency and number increased by 72 hr and further increased by 96 hr of switching to a HFD (Figure 5C). However, after prolonged HFD feeding (12 weeks to 8 months) when obesity is established, the proportion of AT1-ILCs within the lymphoid compartment cells was decreased (Figures 5D and S3A). We then examined the response of AT1-ILCs to weight loss in mice. We removed the HFD from obese mice with established obesity (8 weeks HFD) and replaced it with a standard fat diet (SFD) for 4 weeks. As expected, the mice lost significant body and fat pad weight and AT1-ILCs were restored to the normal frequency (Figure 5D). Thus, AT1-ILC levels rapidly responded to changes in diet, weight loss, and weight gain in mice and humans.

As AT1-ILCs increased at the beginning of HFD feeding (Figure 5C), we next examined whether this increase was due to local proliferation or to infiltration from the periphery. We generated parabiotic mice as before, but this time, we fed one group a HFD for 7 days (starting 7 days after surgery) and the other group only a SFD. We also injected BrdU into each parabiotic mouse in the pair in both the SFD and HFD groups, every 48 hr for the duration of the experiment (Figure 5E). In the HFD group, AT1-ILCs significantly increased (Figure S3B), illustrating that HFD feeding has a similar impact after parabiotic surgery as in non-parabiotic WT mice. AT1-ILC chimerism was also increased, illustrating that HFD feeding induced NK cell infiltration from the periphery (Figure 5F). To rule out the possibility that only infiltrated cells may have proliferated, which would lead to the appearance of increased chimerism, we measured BrdU incorporation in the CD45.1 and CD45.2 AT1-ILCs during the course of parabiosis. We found similar percentages of proliferating AT1-ILCs in SFD- or HFD-fed mice (Figure S3C). However, the number of AT1-ILCs proliferating was increased, due to the increase in total number of AT1-ILCs after HFD (Figure 5G). To determine the source of the proliferating AT1-ILCs, total BrdU^{+} T1-ILCs were gated, and their origin (CD45.1 or CD45.2 derived) was analyzed. In both SFD- and HFD-fed mice, the majority of proliferating AT1-ILCs were not partner derived, suggesting that they were endogenous, although infiltrating T1-ILCs also proliferated in situ in adipose tissue (Figure S3D). There was no difference between the proportions of endogenous versus infiltrating T1-ILCs that were proliferating between the SFD or HFD pairs (Figure S3D, right). As a control, we also measured T1-ILC levels and chimerism in blood. There was an increase in circulating T1-ILC levels in parabiotic pairs under this short-term HFD (Figure S3E), but no difference in chimerism (Figure S3F), suggesting that the increased infiltrating AT1-ILCs in HFD come from an increased pool in the periphery. Taken together, using parabiosis in diet-induced obesity models for the first time, we show that T1-ILCs infiltrate into adipose tissue at onset of obesity. While infiltration was the primary source of the increase in AT1-ILCs, there was also an increase in the number of proliferating AT1-ILCs, which together with increased infiltration cumulatively accounted for increase in AT1-ILCs in adipose tissue during HFD feeding.

As the AT1-ILCs population comprises three phenotypically and functionally distinct subsets, some of which are unique to AT and have distinct trafficking patterns, we next asked whether they had a differential response to obesity. We found a significant increase in the proportion of the mNK cell subset after

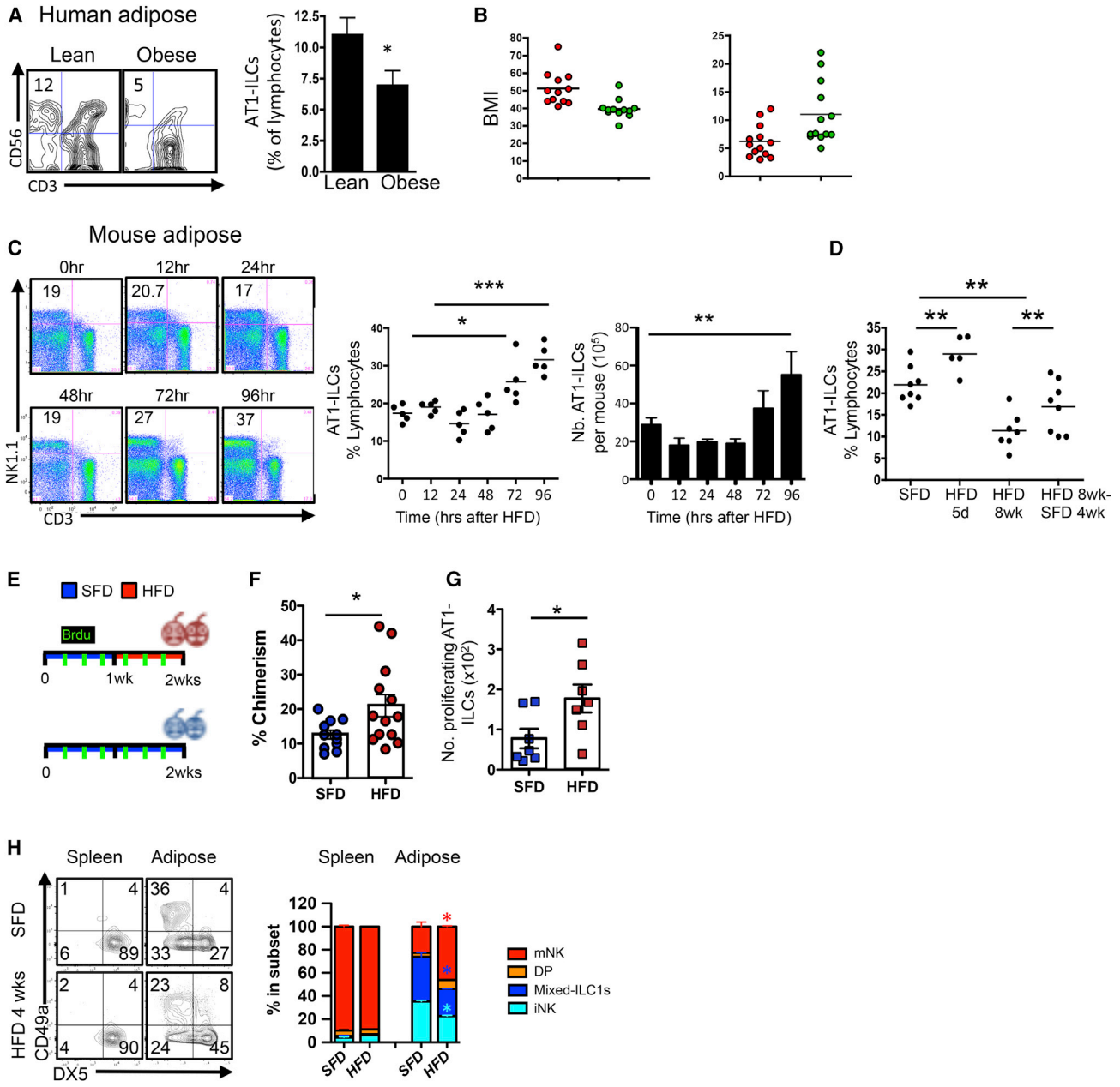

Figure 5. T1-ILCs Have a Dynamic Response to Weight Gain and Loss in Mice and Humans

(A) Representative cytometry contour plots (left) and quantitation (right) of T1-ILC percentages in human adipose from lean and obese individuals.

(B) Body mass index (BMI, left), at pre- and post-bariatric surgery. Middle: percent of peripheral blood T1-ILCs in cross-sectional (n = 12–15 unmatched patients) and longitudinal (right, n = 6 matched patients, paired t test) studies.

(C) Representative cytometry plots of epididymal AT1-ILCs from HFD time course of 0 hr (SFD) to 12, 24, 36, 48, 72, and 96 hr of HFD, and AT1-ILC levels (middle) and numbers (right) from each mouse during HFD.

(D) Percentages of AT1-ILCs of lean (SFD), short-term (5 days) and long-term (8 weeks) HFD, and after 4 weeks of returning to SFD after 8 weeks of feeding with HFD (n = 5–8 per group, unpaired t test).

(E) Diagram of experimental set up to study T1-ILC circulation and proliferation at the onset of obesity. Schematic: Parabiotic pairs were fed a SFD for 3 days, then HFD for 2 weeks (top), compared to SFD (bottom). BrdU was i.p. injected on day 1 after surgery and every second day for 2 weeks.

(F and G) Quantitation of level of chimerism (F) and number of proliferating ILC1s (G) (see Figures S3B–S3F).

(H) Cytometry contour plot (left) and proportions (right) of T1-ILC subsets in spleen and adipose from SFD- and HFD (4 weeks)-fed mice (n = 2–3 mice per group, 2 independent experiments).

Error bars represent SEM. Statistical comparisons using unpaired two-tailed Student's t test. *$p < 0.05$, **$p \leq 0.01$, ***$p < 0.001$. See also Figure S3.

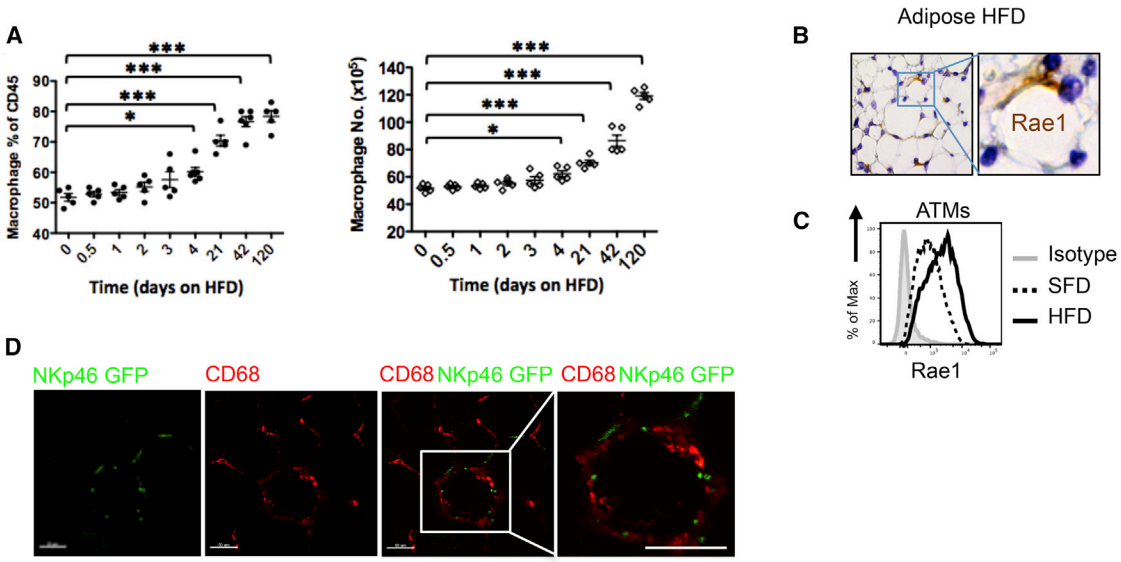

Figure 6. ATMs Express Stress Ligands at Steady State and in Obesity and Interact with AT1-ILCs

(A) ATM levels as a percentage of CD45$^+$ cells (left) and numbers (right) after early and prolonged HFD intake (~120 days). Macrophages were gated as CD45$^+$F480$^+$CD11b$^+$ and levels measured as a percent of CD45$^+$ cells.

(B) Rae1 immunostaining of white adipose tissue.

(C) Cytometry histograms of Rae1 expression in F4/80$^+$ adipose macrophages in SFD and HFD (8 weeks) mice.

(D) Immunofluorescence staining of adipose tissue from *Ncr1*$^{+/gfp}$ mice showing close contact (arrowhead) of NKp46$^+$ NK cells (green) and CD68$^+$ macrophages (red).

HFD, in agreement with our conclusion that the increase in total AT1-ILCs in obesity accounts mostly from infiltration of mNK cells from the periphery (Figure 5H). As a result, there was a decrease in the proportion of the tissue-resident AT1-ILC subsets (DP, iNK, and mixed ILC1s) after HFD. Similar observations were made in BAT and subcutaneous (Sub-C) adipose (Figure S3G).

Taken together, our data show that AT1-ILC levels and dynamics are rapidly altered by changes of diet; mNK cells infiltrate adipose tissue at the onset of obesity, and the overall AT1-ILCs are later decreased after chronic obesity but can be restored to normal levels with weight loss.

ATMs Express Stress Ligands at Steady State and during Obesity

Obesity-induced inflammation is associated with aberrant ATM expansion (Amano et al., 2014). By tracking ATM kinetics in HFD-fed mice, we found that ATMs, like AT1-ILCs, quickly respond to HFD. Unlike AT1-ILCs, ATMs keep expanding after prolonged HFD (Figure 6A). Obesity-induced inflammation is partly due to the adipose stress response to excess energy intake and storage. We looked for stress signals that T1-ILCs including NK cells would recognize. By immunohistochemistry, we detected Rae-1$^+$ cells in obese adipose tissue (Figure 6B). Rae-1 is an NKG2D ligand upregulated in stressed cells, making them potential targets of NK cell cytotoxicity (Raulet et al., 2013). By flow cytometry, we found that ATMs were the main cell expressing Rae-1 at steady state in lean adipose tissue (Figure 6C), which was unusual as these stress ligands are not typically expressed at steady state. Furthermore, Rae1 levels were increased on ATMs during HFD. NK cells can interact with macrophages through NKG2D-Rae1 during infection or LPS-induced inflammation (Raulet et al., 2013). By confocal microscopy and using NKp46-GFP reporter mice (*Ncr1*^{gfp}), we observed that AT1-ILCs and adipose macrophages (CD68$^+$) were both distributed around adipocytes and in most cases were proximal to each other (Figure 6D), suggesting that they may interact at steady state.

AT1-ILCs Are Necessary and Sufficient for Regulating ATM Homeostasis through Targeted Cytotoxicity

Given the expression of stress ligands on ATMs, we asked whether AT1-ILCs might kill ATMs. We sorted and co-cultured autologous AT1-ILCs and ATMs from lean mice. Interestingly, AT1-ILCs killed macrophages from lean mice ex vivo, in a dose-dependent manner, as measured by the number of dead macrophages and the degranulation of AT1-ILCs (Figures 7A and S4A). AT1-ILCs killed M2 macrophages more effectively than M1 (Figure 7B). We reasoned that if a physiological role of AT1-ILCs involved regulation of macrophages through directed cytotoxicity, then depleting AT1-ILCs should affect ATM homeostasis. To test this, we depleted AT1-ILCs by anti-asialo GM1 (aGM1) injections for 1 week. aGM1 was used as anti-NK1.1 can also deplete iNKT cells, and anti-aGM1 uniformly ablated all AT1-ILCs (Figure S4B). Depletion of AT1-ILCs resulted in a significant increase in ATM number and proportion (Figure 7C). Importantly, a significant increase in M2 macrophages accounted for most of the increased ATMs (Figure 7D). The surface expression of stress ligands Rae1 in ATMs at steady state prompted the question of whether ATM killing was NKG2D dependent. We found a trend in decreased M1 levels ($p = 0.06$) and an increase in M2:M1 ratio ($p = 0.07$) in NKG2D-deficient

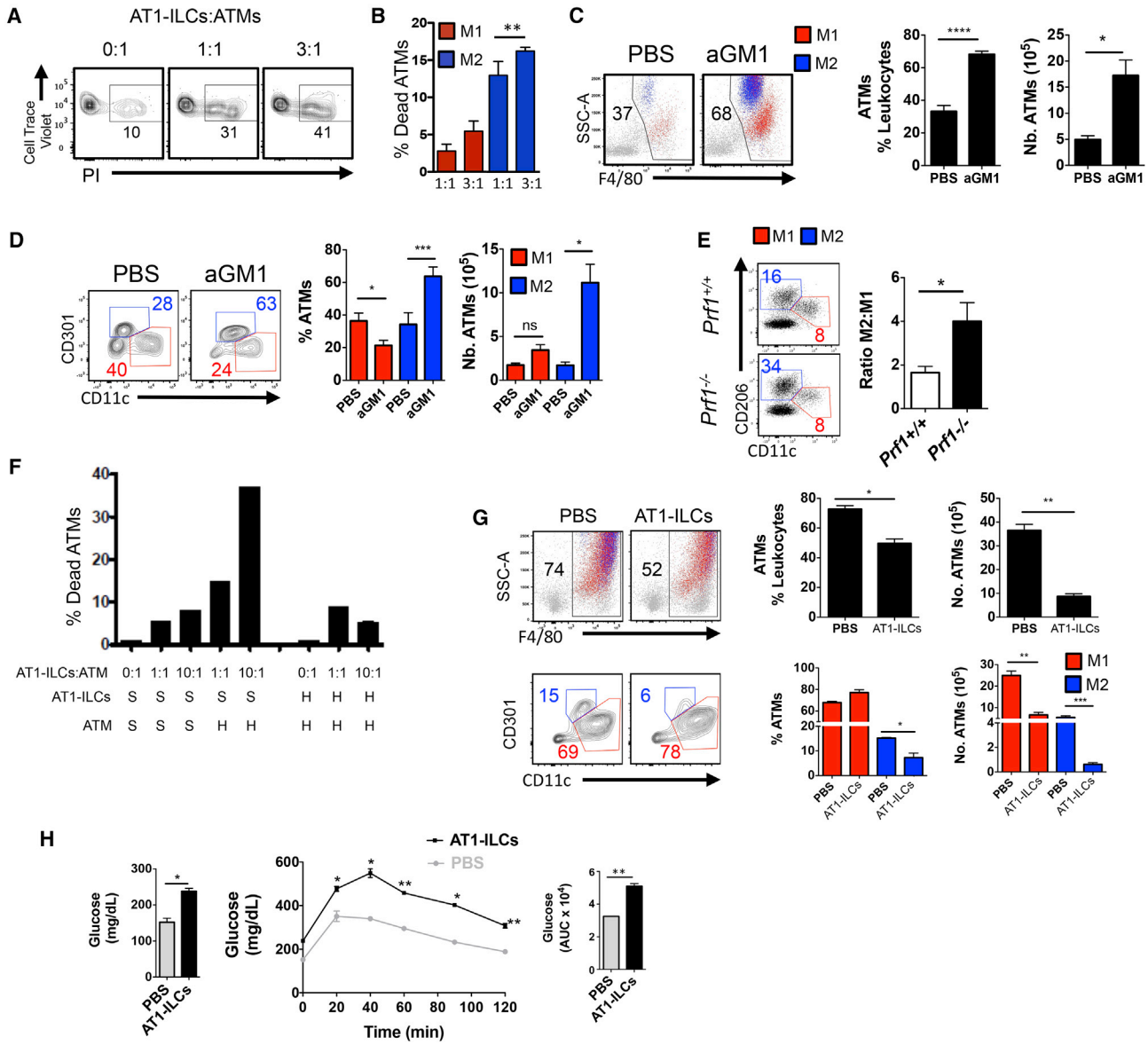

Figure 7. AT1-ILCs Are Necessary and Sufficient for Homeostasis ATMs

(A and B) Representative contour cytometry plots of total ATMs stained with PI (A) and percent of dead ATMs after co-incubation with autologous AT1-ILCs at the indicated ratios (B) (n = 10 mice, 2–3 biological replicates, 3 experiments).

(C) Cytometry dot plots and quantifications of total ATMs in AT1-ILCs depleted with anti-asialo GM1 (aGM1) and PBS control mice.

(D) Contour plots and quantification of M1 and M2 of ATMs in SFD mice after AT1-ILC depletion with aGM1 (n = 3–7 mice per group, two experiments).

(E) Representative dot plot and calculation of M2:M1 ratio in SFD-fed *Pfr1*$^{-/-}$ and *Prf1*$^{+/+}$ mice.

(F) Representative cytotoxic assay with adipose AT1-ILCs co-incubated with ATMs target cells from either SFD-fed (S) or HFD-fed (H) mice at the indicated AT1-ILC:ATM ratios (n = 10 mice per group, two independent experiments).

(G) Representative cytometry plots and quantification of total ATMs and gated M1 (red) and M2 (blue) in obese mice adoptively transferred with total lean-derived AT1-ILCs (n = 2–3 injected mice per group with n = 10 donor mice, two independent experiments).

(H) Fasting blood glucose (right), glucose test tolerance (middle), and area under the curve (AUC, right) of adoptively obese WT mice after adoptive transfer of total AT1-ILC subsets derived from WT lean donor mice or PBS.

Error bars represent SEM. Statistical comparisons using unpaired two-tailed Student t test. *p < 0.05, **p ≤ 0.01, ***p < 0.001. See also Figure S4.

(*Klrk1*$^{-/-}$) compared to NKG2D-sufficient (*Klrk1*$^{+/+}$) lean mice (Figure S4C). Similar results were obtained in obesity settings (Chung et al., 2014). Thus we conclude that expression of NKG2D stress ligands on ATMs may play an important role, but NKG2D-ligand interaction may be redundant in regulating ATM homeostasis and other pathways may be involved. To validate the importance of cytotoxicity in regulating ATM levels at steady state, we examined ATM in perforin-deficient mice

(*Prf1*$^{-/-}$). The AT1-ILC compartment was normal in *Prf1*$^{-/-}$ mice (Figure S4D). Similar to AT1-ILC-depleted mice, the levels of M2 macrophages were increased in *Prf1*$^{-/-}$ mice leading to a significantly greater M2:M1 ratio, compared to *Prf*$^{+/+}$ mice (Figure 7E). Thus, AT1-ILCs have the ability to kill macrophages in adipose tissue at steady state, particularly M2 macrophages, and this is important for ATM homeostasis.

Obesity Interferes with AT1-ILC Cytotoxicity

We have shown that AT1-ILCs are reduced in established obesity in humans (Figure 5A) and mice (Figure 5D). We hypothesized that reduced levels of AT1-ILCs and/or their functional defect in cytotoxicity in obesity may play a role in ATM expansion in obesity. To explore this, we performed cytotoxicity assays with isolated AT1-ILCs and ATMs from SFD (S)- or HFD (H)-fed mice (Figure 7F). As shown before, AT1-ILCs from SFD-fed mice killed ATMs from SFD-fed mice, but killed ATMs from HFD more effectively. However, AT1-ILCs from obese mice had significantly reduced ability to kill ATMs from HFD-fed mice, suggesting that prolonged obesity may impair their killing capacity. As well as infiltration, ATMs have been shown to proliferate in situ, which is enhanced in obesity (Amano et al., 2014). Once again, we found that depleting AT1-ILCs caused a dramatic increase in proliferating ATMs in lean mice. However, in obese mice, depleting AT1-ILCs did not affect ATM proliferation, also suggesting that AT1-ILCs lose their ability to regulate ATMs in obesity (Figure S4E). Finally, we investigated whether AT1-ILCs from lean mice were sufficient to reduce ATMs in HFD-fed obese mice. Adoptive transfer of AT1-ILCs from lean mice into obese mice resulted in a significant reduction in ATM levels and numbers (Figure 7G, top). The effects of adoptive transfer of AT1-ILCs reduced both M1 and M2 numbers, but the effects on M2 macrophages were more pronounced and resulted in a significant increase in the M1:M2 ratio (Figure 7G, bottom). Thus, our findings show that AT1-ILCs are necessary and sufficient for maintaining ATMs homeostasis at steady state but during obesity, this cytotoxic regulatory function is lost, which may account for the uncontrolled expansion of ATMs.

As AT1-ILCs comprise at least three subsets, we next investigated whether one or more subset could kill ATMs. We cell sorted CD49a^{+} mixed ILC1, iNK cell, and mNK cell subsets from WT lean donor mice and adoptively transferred equal numbers of each subset into recipient obese mice. All AT1-ILC subsets could reduce ATM frequencies and numbers in vivo in obese mice, albeit to slightly different degrees (Figure S4F, left). Both M1 and M2 macrophages were reduced in number, agreeing with our findings that AT1-ILCs can kill both M1 and M2 macrophages (Figure S4F, right). Transfer of all AT1-ILC subsets resulted in reduced M2 numbers in adipose tissue, although with slightly differing levels; iNK cell transfer results in the bigger reduction in both M1 and M2 macrophages, while transfer of mNK cells impacted ATMs to a lesser extent. We also tested the killing ability of each AT1-ILC subset in vitro against autologous ATMs from lean mice. Again, all AT1-ILC subsets could kill autologous ATM in vitro, and iNK cells were the most efficient killers (Figure S4G). These subsets also had the highest level of degranulation (Figure S4H). Given that transfer of all AT-ILCs increases the M1:M2 ratio in adipose tissue, their depletion increases M2 macrophages in adipose tissue and each subset produces IFN-γ, so we hypothesized that this would negatively impact systemic metabolism. Fasting blood glucose levels and impaired glucose handling were significantly higher in mice that received total AT1-ILCs compared to vehicle alone (Figure 7H). Our results agree with the link between AT1-ILCs and metabolic homeostasis recently reported. We also highlight subtle differences in the contribution of each subset to macrophage homeostasis, although the net effect of AT1-ILCs is targeted cytotoxicity against macrophages, particularly of the M2 phenotype, and production of IFN-γ. Together, we demonstrate unique functions of AT1-ILCs in regulating ATM homeostasis at steady state and we propose that obesity-associated loss of cytotoxic function accounts for ATM accumulation and glucose intolerance.

DISCUSSION

Innate lymphoid cells (ILCs), including NK cells, are important regulators of tissue homeostasis, inflammation, and repair (Diefenbach et al., 2014). Here we identified unique AT1-ILC subsets in human and mouse adipose tissue. In mice, AT1-ILCs included circulating mNK cells while the majority were tissue-resident iNK and CD49a^{+} mixed ILC1 subsets. We found that AT1-ILCs and macrophages interact in adipose tissue, which resulted in ATM death and homeostatic regulation at steady state. Indeed, adoptive transfers or depletion of T1-ILCs show that NK cells are necessary and sufficient to regulate macrophage homeostasis. Our data show a new mechanism by which macrophages are kept in check by AT1-ILC cytotoxicity to prevent aberrant expansion. In chronic obesity, AT1-ILCs were decreased in numbers and their killing ability against ATMs in vitro was significantly impaired. This loss of function may be at least partly responsible for the increase in macrophages associated with obesity, as transfer of "lean" AT-ILC1 subsets were sufficient to reduce adipose macrophages number and frequency in obesity. Taken together, our data suggest that regulating ATM homeostasis is a key role of AT1-ILCs.

Interestingly, within the three AT1-ILC subsets, the expression of Eomes did not correlate with DX5 or CD49a expression, and the CD49a^{+} subset (identified as mixed ILC1s) was composed of Eomes^{-} ILC1s and Eomes^{+} iNK cells. Using *Eomes* reporter mice, similar AT1-ILC subsets were recently characterized (O'Sullivan et al., 2016). However, by analyzing the requirement of Tbet for AT1-ILC subsets using a different gating strategy, we found that the presence of CD49a^{+} was maintained independently of *Tbx21* and that this population was composed of Eomes^{+} iNK cells. This suggests that iNK cells could acquire ILC1 attributes to preserve this CD49a^{+} compartment when compensation is required. In addition, the residency of some AT1-ILCs was not exclusively tied to CD49a expression. Instead, iNK cells were CD49a^{-} but were mainly tissue resident in our parabiosis experiments. Adipose CD49a^{+} mixed ILC1s expressed the most IFN-γ, the least granzyme B, and no TRAIL, unlike ILC1s in liver. In humans, visceral omental adipose tissue showed a similar enrichment of an unconventional CD16^{-}CD56^{lo}CD127^{lo} ILC1-like population with low expression of cytotoxic molecules. In human adipose, peripheral-like CD16^{+}CD56^{lo} were found at low levels and CD16^{-}CD56^{bright} CD127^{+} cells were virtually absent. The question of whether these

adipose ILC1-like subsets are developmental intermediates undergoing ILC1 or NK cell conversion needs further investigation, but we have described distinct populations with specific effector molecules, found in all patients regardless of age or BMI, suggesting that AT1-ILC subsets have specific functions distinct from peripheral conventional NK cells.

We found that AT1-ILCs rapidly respond to changes in diet, in both human and mice. iNKT are also tissue resident in adipose and they dramatically decreased in human and murine obesity (Lynch et al., 2009a, 2012). Here, we showed by parabiosis that peripheral T1-ILC levels rapidly increased in blood and infiltrate adipose tissue within the first days of starting HFD in mice. This dynamic response is similar to that of monocyte and macrophage infiltration to adipose tissue in early-stage obesity. However, there were some differences between the macrophage and T1-ILC response; while macrophages continue to accumulate in adipose tissue throughout obesity, the overall percentage of total AT1-ILCs is decreased in both humans and mice during prolonged obesity. We also found that blood and adipose T1-ILCs were able to reverse to normal levels upon weight loss in both humans and mice, revealing that AT1-ILCs are dynamic diet or energy sensors. Recent studies reported a negative impact of AT1-ILCs on metabolic health and accounted this effect to AT1-ILC-induced promotion of M1 expansion (Lee et al., 2016; Wensveen et al., 2015). Two studies found that this was through increased production of IFN-γ by AT1-ILCs in obesity (O'Sullivan et al., 2016; Wensveen et al., 2015), while the other study found no increase in IFN-γ but rather an increase in TNF-α production by AT1-ILCs in HFD (Lee et al., 2016). We also observed a decrease in percentage of pro-inflammatory M1 macrophages in AT1-ILC-depleted mice in agreement with the previous studies (O'Sullivan et al., 2016; Wensveen et al., 2015). However, given the effect of AT1-ILCs on macrophage killing, it is possible that the effects of AT1-ILCs on M1 macrophages are secondary or complimentary to the direct effects of AT1-ILC killing of macrophages, primarily M2 macrophages. T1-ILCs can kill M2 macrophages in other circumstances, while M1 macrophages are resistant to T1-ILC cytotoxicity (Bellora et al., 2010). Nevertheless, our data revealed an unexpected finding, as the dogma states that M2 macrophages have many beneficial effects on tissue homeostasis and dampening inflammation (Fischer-Posovszky et al., 2011). Thus, it is puzzling as to why they would be targets of AT1-ILC cytotoxicity, naturally, without infection or HFD or changes in surface expression of MHC class I (not shown). One possibility is that M2 macrophages are very active in lean adipose tissue, remodeling and surveying for dying adipocytes or other potential hazardous extracellular material to engulf. Once they have fulfilled their role in buffering from potentially dangerous material, they may upregulate "kill me" signals to prevent inflammation. Thus the T1-ILC-M2 macrophage relationship may play an important homeostatic role in preventing the development of stressed pro-inflammatory macrophages in adipose tissue. However, obesity may override this system, with the loss of AT1-ILCs within the adipose lymphoid compartment, the loss of their killing potential, and the dysregulation of macrophages. On the other hand, upregulation of AT1-ILCs-obese-derived IFN-γ may further contribute to insulin resistance. Here, by studying the metabolic outcome of lean-derived AT1-ILCs that are still competent for both killing potential and IFN-γ production at physiological level, we found that the AT1-ILC cytotoxicity resulted in reduced M2 macrophages and more severe glucose intolerance. Thus, we propose a novel "physiological killing" of macrophages by adipose AT1-ILCs to maintain adipose homeostasis at steady state, hereby highlighting the importance of understanding ILC and macrophage interactions in health and disease.

EXPERIMENTAL PROCEDURES

Mice

Male (and where indicated, female) wild-type (WT) C57BL/6, *Tbx21*$^{-/-}$ (Finotto et al., 2002), *Pfrn*$^{-/-}$ (C57BL/6-Prf1$^{tm1Sdz/J}$ [Kägi et al., 1994]), and *Ifng*$^{yfp/yfp}$ (GREAT/*Ifng*$^{tm3(EYFP)Lky}$ [Reinhardt et al., 2009]) mice were purchased from Jackson Laboratories. *Nfil3*$^{-/-}$ mice (Kamizono et al., 2009) were a kind gift from Dr. Vijay Kuchroo. Where indicated, mice received either SFD or HFD (Research Diets, 60 kcal% fat) from 6 weeks of age. Mice were housed under specific-pathogen-free conditions. Animal experiments were performed in accordance with protocols approved by the Institutional Animal Care and Use Committee.

Subjects

10 mL of peripheral blood and visceral fat was obtained from obese subjects undergoing bariatric surgery (mean BMI 48) and from ex-obese undergoing plastic surgery after weight loss. Visceral, subcutaneous, mesenteric, and peri-colic fat was also obtained from eight lean patients undergoing abdominal surgery (two hernia repair, one rectal prolapse, and five resections). For cross-sectional and longitudinal studies, we collected blood from a group of 12 obese patients before and 12 patients 18 months after bariatric surgery, and we followed 6 individuals before and 12 patients 18 months after bariatric surgery and collected their blood and BMI at these time points. All blood samples were obtained with written informed consent. The ethics committee at Brigham and Women's Hospital, Boston, and St. Vincent's University Hospital, Dublin, granted approval for this study.

Cell Preparation

Adipose tissue was processed as previously described (Lynch et al., 2015) to obtain a cell suspension of stromovascular cells (SVF). A detailed description and staining reagents and procedures are detailed in the Supplemental Experimental Procedures.

Parabiotic Surgery

Parabiosis was performed as previously described (Lynch et al., 2015) using CD45.1$^+$ and CD45.2$^+$ mice. Parabiotic mice were kept together for 2–3 weeks. One group received HFD for 2 weeks. Chimerism in the blood and tissues was defined as the percent CD45.1$^+$ cells over the percent of CD45.1$^+$ cells and vice versa.

Killing Assays

Sorted macrophages were plated and labeled with Cell Trace Violet and sorted adipose NK cells were added at the indicated effector:target (E:T) ratios. After 4 hr of co-incubation, propidium iodide was added to discriminate dead target cells (macrophages), analyzed by flow cytometry.

Type 1 ILC Depletion

Anti-mouse Asialo GM1 (Ganglioside, ganglio-N-tetraosylceramide, clone Poly21460, Biolegend) or PBS vehicle was i.p. injected to WT mice at 40 μL per mouse every 2 days for a duration of 8 days.

Adoptive Transfer

50,000 sorted WT lean-derived AT1-ILCs (live CD45$^+$NK1.1$^+$CD3$^-$ singleton lymphocytes) or 20,000 individual WT lean-derived AT1-ILC subsets—mNK (DX5$^+$CD49a$^-$), iNK (DX5$^-$CD49a$^-$), or mixed-ILC1 (DX5$^-$CD49a$^+$)—were i.p. injected in 100 μL of PBS to HFD-fed mice. PBS vehicle was similarly injected as negative control.

Glucose Tolerance Test

After 6 hr of fasting, mice were injected with 1 g glucose per kg body intraperitoneally (i.p.), and glucose levels were measured before and every 20 min for 120 min after injection using an automated glucometer (LifeScan).

Statistics

Error bars represent SEM. The statistical significance of differences between two groups was determined using the Mann-Whitney U test or Student's t tests where appropriate after determination of Gaussian distribution of the data, or by one-way ANOVA for groups of more than two, with Tukey post hoc test.

SUPPLEMENTAL INFORMATION

Supplemental Information includes four figures and Supplemental Experimental Procedures and can be found with this article online at http://dx.doi.org/10.1016/j.immuni.2017.01.008.

AUTHOR CONTRIBUTIONS

L.L. and S.B. designed and performed experiments, analyzed data, and wrote the paper; A.E.H. and D. O'Shea performed the human weight loss work; X.M., D.D., C.D., D.A., D. O'Connor, and S.S. performed experiments; A.T. and D.W. enabled human adipose studies; and M.A.E., M.B.B., and U.v.A. contributed to the design of experiments and provided materials and tools.

ACKNOWLEDGMENTS

L.L. was supported by an American Diabetes JF Development Award (116JDF061), a BWH Evergreen Innovation Grant, a BADERC grant, and an ERC Stg grant (679173). S.B. is supported by Wallonie Bruxelles International Award. M.B.B. is supported by NIH 5RO1AI113046. U.v.A. is supported by HMS Center for Immune Imaging and PO1 AI112521.

Received: May 18, 2016
Revised: October 24, 2016
Accepted: January 9, 2017
Published: February 21, 2017

REFERENCES

Amano, S.U., Cohen, J.L., Vangala, P., Tencerova, M., Nicoloro, S.M., Yawe, J.C., Shen, Y., Czech, M.P., and Aouadi, M. (2014). Local proliferation of macrophages contributes to obesity-associated adipose tissue inflammation. Cell Metab. *19*, 162–171.

Bellora, F., Castriconi, R., Dondero, A., Reggiardo, G., Moretta, L., Mantovani, A., Moretta, A., and Bottino, C. (2010). The interaction of human natural killer cells with either unpolarized or polarized macrophages results in different functional outcomes. Proc. Natl. Acad. Sci. USA *107*, 21659–21664.

Bernink, J.H., Peters, C.P., Munneke, M., te Velde, A.A., Meijer, S.L., Weijer, K., Hreggvidsdottir, H.S., Heinsbroek, S.E., Legrand, N., Buskens, C.J., et al. (2013). Human type 1 innate lymphoid cells accumulate in inflamed mucosal tissues. Nat. Immunol. *14*, 221–229.

Bernink, J.H., Krabbendam, L., Germar, K., de Jong, E., Gronke, K., Kofoed-Nielsen, M., Munneke, J.M., Hazenberg, M.D., Villaudy, J., Buskens, C.J., et al. (2015). Interleukin-12 and -23 control plasticity of CD127(+) group 1 and group 3 innate lymphoid cells in the intestinal lamina propria. Immunity *43*, 146–160.

Björkström, N.K., Ljunggren, H.-G., and Michaëlsson, J. (2016). Emerging insights into natural killer cells in human peripheral tissues. Nat. Rev. Immunol. *16*, 310–320.

Boulenouar, S., Doisne, J.M., Sferruzzi-Perri, A., Gaynor, L.M., Kieckbusch, J., Balmas, E., Yung, H.W., Javadzadeh, S., Volmer, L., Hawkes, D.A., et al. (2016). The residual innate lymphoid cells in NFIL3-deficient mice support suboptimal maternal adaptations to pregnancy. Front. Immunol. *7*, 43.

Brestoff, J.R., and Artis, D. (2015). Immune regulation of metabolic homeostasis in health and disease. Cell *161*, 146–160.

Brestoff, J.R., Kim, B.S., Saenz, S.A., Stine, R.R., Monticelli, L.A., Sonnenberg, G.F., Thome, J.J., Farber, D.L., Lutfy, K., Seale, P., and Artis, D. (2015). Group 2 innate lymphoid cells promote beiging of white adipose tissue and limit obesity. Nature *519*, 242–246.

Chiossone, L., Chaix, J., Fuseri, N., Roth, C., Vivier, E., and Walzer, T. (2009). Maturation of mouse NK cells is a 4-stage developmental program. Blood *113*, 5488–5496.

Chung, J.J., Markiewicz, M.A., Polić, B., and Shaw, A.S. (2014). Role of NKG2D in obesity-induced adipose tissue inflammation and insulin resistance. PLoS ONE *9*, e110108.

Cortez, V.S., and Colonna, M. (2016). Diversity and function of group 1 innate lymphoid cells. Immunol. Lett. *179*, 19–24.

Cortez, V.S., Fuchs, A., Cella, M., Gilfillan, S., and Colonna, M. (2014). Cutting edge: Salivary gland NK cells develop independently of Nfil3 in steady-state. J. Immunol. *192*, 4487–4491.

Cortez, V.S., Cervantes-Barragan, L., Robinette, M.L., Bando, J.K., Wang, Y., Geiger, T.L., Gilfillan, S., Fuchs, A., Vivier, E., Sun, J.C., et al. (2016). Transforming growth factor-β signaling guides the differentiation of innate lymphoid cells in salivary glands. Immunity *44*, 1127–1139.

Daussy, C., Faure, F., Mayol, K., Viel, S., Gasteiger, G., Charrier, E., Bienvenu, J., Henry, T., Debien, E., Hasan, U.A., et al. (2014). T-bet and Eomes instruct the development of two distinct natural killer cell lineages in the liver and in the bone marrow. J. Exp. Med. *211*, 563–577.

Diefenbach, A., Colonna, M., and Koyasu, S. (2014). Development, differentiation, and diversity of innate lymphoid cells. Immunity *41*, 354–365.

Exley, M.A., Hand, L., O'Shea, D., and Lynch, L. (2014). Interplay between the immune system and adipose tissue in obesity. J. Endocrinol. *223*, R41–R48.

Feuerer, M., Herrero, L., Cipolletta, D., Naaz, A., Wong, J., Nayer, A., Lee, J., Goldfine, A.B., Benoist, C., Shoelson, S., and Mathis, D. (2009). Lean, but not obese, fat is enriched for a unique population of regulatory T cells that affect metabolic parameters. Nat. Med. *15*, 930–939.

Finotto, S., Neurath, M.F., Glickman, J.N., Qin, S., Lehr, H.A., Green, F.H., Ackerman, K., Haley, K., Galle, P.R., Szabo, S.J., et al. (2002). Development of spontaneous airway changes consistent with human asthma in mice lacking T-bet. Science *295*, 336–338.

Fischer-Posovszky, P., Wang, Q.A., Asterholm, I.W., Rutkowski, J.M., and Scherer, P.E. (2011). Targeted deletion of adipocytes by apoptosis leads to adipose tissue recruitment of alternatively activated M2 macrophages. Endocrinology *152*, 3074–3081.

Gordon, S.M., Chaix, J., Rupp, L.J., Wu, J., Madera, S., Sun, J.C., Lindsten, T., and Reiner, S.L. (2012). The transcription factors T-bet and Eomes control key checkpoints of natural killer cell maturation. Immunity *36*, 55–67.

Hotamisligil, G.S., Shargill, N.S., and Spiegelman, B.M. (1993). Adipose expression of tumor necrosis factor-alpha: direct role in obesity-linked insulin resistance. Science *259*, 87–91.

Ji, Y., Sun, S., Xu, A., Bhargava, P., Yang, L., Lam, K.S., Gao, B., Lee, C.H., Kersten, S., and Qi, L. (2012). Activation of natural killer T cells promotes M2 macrophage polarization in adipose tissue and improves systemic glucose tolerance via interleukin-4 (IL-4)/STAT6 protein signaling axis in obesity. J. Biol. Chem. *287*, 13561–13571.

Kägi, D., Ledermann, B., Bürki, K., Seiler, P., Odermatt, B., Olsen, K.J., Podack, E.R., Zinkernagel, R.M., and Hengartner, H. (1994). Cytotoxicity mediated by T cells and natural killer cells is greatly impaired in perforin-deficient mice. Nature *369*, 31–37.

Kahn, B.B., and Flier, J.S. (2000). Obesity and insulin resistance. J. Clin. Invest. *106*, 473–481.

Kamizono, S., Duncan, G.S., Seidel, M.G., Morimoto, A., Hamada, K., Grosveld, G., Akashi, K., Lind, E.F., Haight, J.P., Ohashi, P.S., et al. (2009). Nfil3/E4bp4 is required for the development and maturation of NK cells in vivo. J. Exp. Med. *206*, 2977–2986.

Kanneganti, T.D., and Dixit, V.D. (2012). Immunological complications of obesity. Nat. Immunol. *13*, 707–712.

Kosteli, A., Sugaru, E., Haemmerle, G., Martin, J.F., Lei, J., Zechner, R., and Ferrante, A.W., Jr. (2010). Weight loss and lipolysis promote a dynamic immune response in murine adipose tissue. J. Clin. Invest. *120*, 3466–3479.

Lapaque, N., Walzer, T., Méresse, S., Vivier, E., and Trowsdale, J. (2009). Interactions between human NK cells and macrophages in response to Salmonella infection. J. Immunol. *182*, 4339–4348.

Lee, B.C., Kim, M.S., Pae, M., Yamamoto, Y., Eberlé, D., Shimada, T., Kamei, N., Park, H.S., Sasorith, S., Woo, J.R., et al. (2016). Adipose natural killer cells regulate adipose tissue macrophages to promote insulin resistance in obesity. Cell Metab. *23*, 685–698.

Lumeng, C.N., Bodzin, J.L., and Saltiel, A.R. (2007). Obesity induces a phenotypic switch in adipose tissue macrophage polarization. J. Clin. Invest. *117*, 175–184.

Lynch, L., O'Shea, D., Winter, D.C., Geoghegan, J., Doherty, D.G., and O'Farrelly, C. (2009a). Invariant NKT cells and CD1d(+) cells amass in human omentum and are depleted in patients with cancer and obesity. Eur. J. Immunol. *39*, 1893–1901.

Lynch, L.A., O'Connell, J.M., Kwasnik, A.K., Cawood, T.J., O'Farrelly, C., and O'Shea, D.B. (2009b). Are natural killer cells protecting the metabolically healthy obese patient? Obesity (Silver Spring) *17*, 601–605.

Lynch, L., Nowak, M., Varghese, B., Clark, J., Hogan, A.E., Toxavidis, V., Balk, S.P., O'Shea, D., O'Farrelly, C., and Exley, M.A. (2012). Adipose tissue invariant NKT cells protect against diet-induced obesity and metabolic disorder through regulatory cytokine production. Immunity *37*, 574–587.

Lynch, L., Michelet, X., Zhang, S., Brennan, P.J., Moseman, A., Lester, C., Besra, G., Vomhof-Dekrey, E.E., Tighe, M., Koay, H.F., et al. (2015). Regulatory iNKT cells lack expression of the transcription factor PLZF and control the homeostasis of T(reg) cells and macrophages in adipose tissue. Nat. Immunol. *16*, 85–95.

Michel, T., Hentges, F., and Zimmer, J. (2013). Consequences of the crosstalk between monocytes/macrophages and natural killer cells. Front. Immunol. *3*, 403.

Nedvetzki, S., Sowinski, S., Eagle, R.A., Harris, J., Vély, F., Pende, D., Trowsdale, J., Vivier, E., Gordon, S., and Davis, D.M. (2007). Reciprocal regulation of human natural killer cells and macrophages associated with distinct immune synapses. Blood *109*, 3776–3785.

O'Sullivan, T.E., Rapp, M., Fan, X., Weizman, O.E., Bhardwaj, P., Adams, N.M., Walzer, T., Dannenberg, A.J., and Sun, J.C. (2016). Adipose-resident group 1 innate lymphoid cells promote obesity-associated insulin resistance. Immunity *45*, 428–441.

Peng, H., Jiang, X., Chen, Y., Sojka, D.K., Wei, H., Gao, X., Sun, R., Yokoyama, W.M., and Tian, Z. (2013). Liver-resident NK cells confer adaptive immunity in skin-contact inflammation. J. Clin. Invest. *123*, 1444–1456.

Raulet, D.H., Gasser, S., Gowen, B.G., Deng, W., and Jung, H. (2013). Regulation of ligands for the NKG2D activating receptor. Annu. Rev. Immunol. *31*, 413–441.

Reinhardt, R.L., Liang, H.E., and Locksley, R.M. (2009). Cytokine-secreting follicular T cells shape the antibody repertoire. Nat. Immunol. *10*, 385–393.

Rosen, E.D., and Spiegelman, B.M. (2014). What we talk about when we talk about fat. Cell *156*, 20–44.

Schipper, H.S., Rakhshandehroo, M., van de Graaf, S.F., Venken, K., Koppen, A., Stienstra, R., Prop, S., Meerding, J., Hamers, N., Besra, G., et al. (2012). Natural killer T cells in adipose tissue prevent insulin resistance. J. Clin. Invest. *122*, 3343–3354.

Seillet, C., and Belz, G.T. (2016). Differentiation and diversity of subsets in group 1 innate lymphoid cells. Int. Immunol. *28*, 3–11.

Serafini, N., Vosshenrich, C.A.J., and Di Santo, J.P. (2015). Transcriptional regulation of innate lymphoid cell fate. Nat. Rev. Immunol. *15*, 415–428.

Sojka, D.K., Plougastel-Douglas, B., Yang, L., Pak-Wittel, M.A., Artyomov, M.N., Ivanova, Y., Zhong, C., Chase, J.M., Rothman, P.B., Yu, J., et al. (2014). Tissue-resident natural killer (NK) cells are cell lineages distinct from thymic and conventional splenic NK cells. eLife *3*, e01659.

Spits, H., Bernink, J.H., and Lanier, L. (2016). NK cells and type 1 innate lymphoid cells: partners in host defense. Nat. Immunol. *17*, 758–764.

Sun, K., Kusminski, C.M., and Scherer, P.E. (2011). Adipose tissue remodeling and obesity. J. Clin. Invest. *121*, 2094–2101.

Vosshenrich, C.A., Samson-Villéger, S.I., and Di Santo, J.P. (2005). Distinguishing features of developing natural killer cells. Curr. Opin. Immunol. *17*, 151–158.

Wensveen, F.M., Jelenčić, V., Valentić, S., Šestan, M., Wensveen, T.T., Theurich, S., Glasner, A., Mendrila, D., Štimac, D., Wunderlich, F.T., et al. (2015). NK cells link obesity-induced adipose stress to inflammation and insulin resistance. Nat. Immunol. *16*, 376–385.

Wu, D., Molofsky, A.B., Liang, H.E., Ricardo-Gonzalez, R.R., Jouihan, H.A., Bando, J.K., Chawla, A., and Locksley, R.M. (2011). Eosinophils sustain adipose alternatively activated macrophages associated with glucose homeostasis. Science *332*, 243–247.

Xu, X., Grijalva, A., Skowronski, A., van Eijk, M., Serlie, M.J., and Ferrante, A.W., Jr. (2013). Obesity activates a program of lysosomal-dependent lipid metabolism in adipose tissue macrophages independently of classic activation. Cell Metab. *18*, 816–830.